Paleomagnetism of Cretaceous red beds from Tadzhikistan and Cenozoic deformation due to India–Eurasia collision

Article *in* Earth and Planetary Science Letters · June 1994

DOI: 10.1016/0012-821X(94)00072-7

CITATIONS
37

READS
62

5 authors, including:

Mikhail Bazhenov
Russian Academy of Sciences
98 PUBLICATIONS **3,688** CITATIONS

SEE PROFILE

Annick Chauvin
Université de Rennes 1
137 PUBLICATIONS **3,015** CITATIONS

SEE PROFILE

Valentin S. Burtman
Russian Academy of Sciences
70 PUBLICATIONS **5,866** CITATIONS

SEE PROFILE

ELSEVIER

Earth and Planetary Science Letters 124 (1994) 1–18

EPSL

Paleomagnetism of Cretaceous red beds from Tadzhikistan and Cenozoic deformation due to India–Eurasia collision

Mikhail L. Bazhenov [a,c,1], Herve Perroud [b], Annick Chauvin [c], Valentin S. Burtman [a], Jean-Charles Thomas [c]

[a] *Geological Institute, Academy of Sciences, Moscow, Russia,*
[b] *Département des Sciences de la Terre, Université de Pau, 64000 Pau, France,*
[c] *Géosciences Rennes, CNRS, Université de Rennes I, 35042 Rennes Cedex, France*

Received April 26, 1993; revision accepted April 5, 1994

Abstract

We have carried out structural and paleomagnetic studies in the Tadzhik depression in order to evaluate the main features of the Alpine tectonics of this area. About 340 cores from 43 sites of Lower Cretaceous red beds were sampled from four different localities in the basin and adjacent ranges. A well-defined component of magnetization (A) of normal polarity with high unblocking temperatures up to 650–670°C was isolated from all the sites. Another component of magnetization (B) with unblocking temperatures between 650 and 680°C was isolated from only fifteen sites; this component is bipolar. The fold test is positive for both components. We believe that component A was acquired during the Cretaceous long interval of normal polarity. Comparison with Eurasian reference data shows significant counterclockwise rotation of a locality close to the Pamir wedge ($R = 51 \pm 5°$) and another counterclockwise rotation from the inner part of the basin ($R = 15 \pm 5°$). No significant rotations are observed at the two other localities on the periphery of the Tadzhik basin.

1. Introduction

Fold belt formation is commonly attributed to collision of lithospheric plates. The Alpine belt is thought to have resulted from Cenozoic collision of the African plate, in the west, and the Indian plate, in the east, with the Eurasia landmass. Indentation of Eurasia by the rigid Indian wedge led to formation of the mountain chains of the Himalayas, Tibet, Hindukush and the Pamirs. It also becomes clear that collision-related deformation has affected a vast area outside the Alpine belt *sensu stricto*. This is recognized as far as South China in the east and as the Baikal rift system in the north [1,2]. However, while some general agreement has already been reached concerning the relationship of Central Asian tectonics with the Eurasia–India collision, the mode and scale of the tectonic processes are far from clear.

The key area is the Tien Shan belt and the deep sedimentary basins which surround the Pamir wedge (Fig. 1). The Tadzhik depression,

[PT]

[1] Now also at Laboratoire de Paleomagnetisme, Institut de Physique du Globe de Paris, 75230 Paris, Cedex 05 France.

SSDI 0012-821X(94)00072-7

just to the west of this wedge, is a basin filled with thick Mesozoic and Cenozoic sediments which were folded and thrust in the Pliocene–Quaternary. Although the general structural pattern follows rather closely the outline of the Pamir wedge, many features of the depression

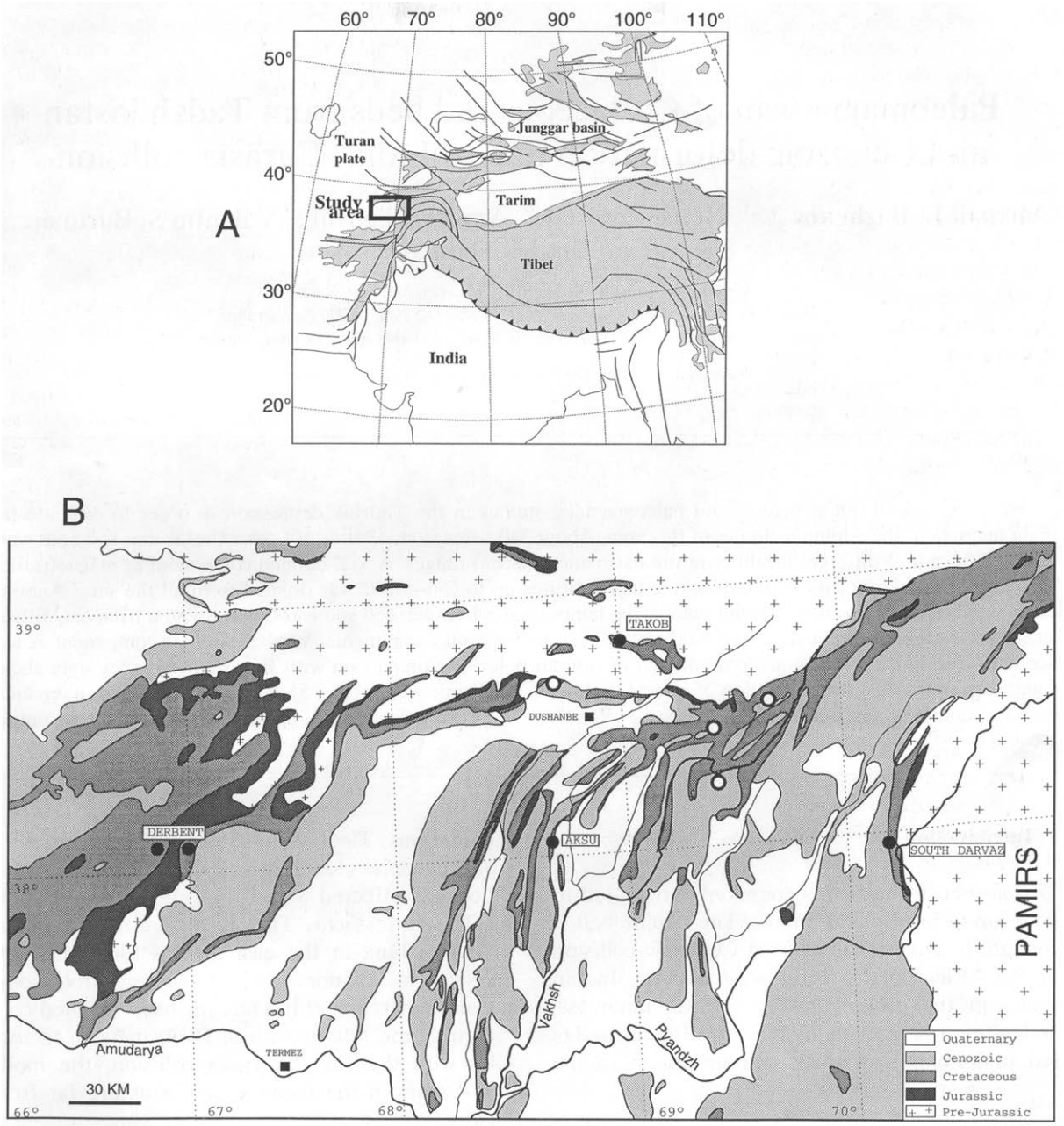

Fig. 1. (A) General location map showing major faults and areas with elevations greater than 2 km (shaded) simplified after Cobbold and Davy [2]. (B) Schematic geological map of the Tadzhik basin, southern Tien Shan and Pamirs. ● = Our sampling localities; ○ = those of Pozzi and Feinberg [5].

tectonics are still debatable, in particular the magnitude of horizontal movements and associated rotations.

Paleomagnetic data may be of great importance in elucidating this problem, and indeed the Cretaceous and Paleogene rocks of the Tadzhik depression, the southern part of the Tien Shan (the Ghissar range) and the westernmost Pamirs have already been studied. The main body of data from the depression and the Ghissar range, however, is based on time-cleaning techniques only [e.g., 3] and thus cannot be considered reliable. In addition, a result from the western border of the Pamirs based on thermal cleaning up to 400°C and a positive fold test [4] is also not of top quality compared to modern standards. Recently, Pozzi and Feinberg [5] presented fully demagnetized data from the northeast Tadzhik basin, but from a limited number of samples.

To study the main features of the Alpine tectonics in both the Tien Shan and Tadzhik depressions, structural and paleomagnetic studies were carried out by French–Soviet expeditions in Kirghizia and Tadzhikistan during the 1989–1990 field seasons. In Tadzhikistan, both Oligocene–Lower Miocene and Lower Cretaceous rocks were sampled at a number of localities. This paper covers the results of the Cretaceous collection.

2. Geological setting and sampling

The Tadzhik basin (depression) is a deep, diamond-shaped basin bounded by the ranges of the Pamirs (the Darvaz and Peter the First ranges) in the east, the Ghissar and southwest Ghissar in the north and west and the mountain chains of Northern Afghanistan in the south (Fig. 1). The basement of the basin has not been reached by the deepest boreholes and has been studied only by geophysical methods; it is thought to be heterogeneous and to comprise strongly deformed Precambrian, Paleozoic and possibly Triassic complexes. The depression is filled with up to 10 km of sediment. The section starts with Lower–Middle Jurassic terrigenous, sometimes coal-bearing rocks, overlain by Upper Jurassic marine limestones, uppermost Jurassic evaporates, Lower Cretaceous red beds (about 1000 m thick) and both marine and continental Upper Cretaceous to Paleogene sediments. An accumulation of several kilometres of conglomerates began around the Oligocene–Miocene boundary and is continuing today. In the adjacent Tien Shan ranges, the Mesozoic and lower Tertiary parts of the section are represented by similar but considerably thinner formations, and the upper Tertiary succession may be still even more reduced or entirely absent.

The main deformation took place in the Pliocene–Quaternary, but weaker unconformities have been recognized in the Lower Miocene [6] and close to the Late Cretaceous–Paleocene boundary [P.R. Cobbold, pers. commun.]. The present geometry and tectonic structure of the depression is thought to have resulted from Alpine deformation. In the east, the shortening of the strongly folded Mesozoic–Cenozoic sedimentary cover in the Peter the First and Transalay ranges occurs between the Pamirs and the Tien Shan. Westward, the depression widens and is characterized by arcuate folds and faults of westward vergence. The magnitude of horizontal displacements is several kilometres at least, and may be much larger. Upper Jurassic evaporates are most probably the main décollement surface judging by large discrepancies in the tectonic patterns above and below them.

We studied Lower Cretaceous red beds (Valanginian to Aptian or Albian [7]) from four localities in the basin itself and in the adjacent ranges (Fig. 1):

(1) The *Derbent* locality is situated to the west of the Tadzhik basin, on the NE–SW trending folds of the southwest Ghissar range. Fourteen sites were drilled at four sections with various bedding attitudes.

(2) The *Aksu* locality is situated on the eastern slope of the Esamol ridge in the north-central part of the depression, about 50 km south of Dushanbe. Seven, six and three sites were sampled on the western and eastern limbs of the large anticline and its axial part respectively. In addition, a large block was taken from a layer of intraformational conglomerate on the western limb. The conglomerate consists of dark red sandstone pebbles (several millimetres in size and

with clearly defined margins) in a paler sandy matrix.

(3) The *Takob* locality is situated to the north of the depression on the southern slope of the Ghissar range, about 30 km north of Dushanbe. Valanginian to Aptian sediments form a syncline with gentle southern and steep northern limbs. Eleven sites were drilled on the southern limb. The same rocks were also sampled along two sections (twelve and thirteen handsamples) on the two limbs of the syncline. The main part of this collection consists of red beds, but several beds of grey sandstones were sampled too.

(4) The *Darvaz* locality is close to the southern termination of the Darvaz range, about 2 km to the west of the Paleozoic Pamir domain. Here, Cretaceous red beds are part of a large N–S striking structure where Upper Jurassic to at least Lower Miocene rocks outcrop without angular unconformities; the beds are vertically dipping or overturned. The previously published result from this locality is based on incomplete demagnetization [4], and we restudied duplicate specimens from fourteen handsamples.

In general, a site covered a layer of apparently uniform lithology up to 5 m along strike and up to 1 m in cross section. Six to nine cores, oriented with solar and magnetic compasses, were drilled at each site. When sampling along sections, handsamples oriented with a magnetic compass were spaced several metres along the sections over a true thickness of several tens to two hundred metres.

3. Measurements and procedures

One specimen from each core and two specimens from each handsample were heated in fifteen steps up to 680°C using the Schonstedt TSD-1 demagnetizer. Six specimens from the conglomerate block were demagnetized. Measurements were made either with a Schonstedt fluxgate magnetometer or with a LETI cryogenic magnetometer. All the data were analyzed with stereonets and orthogonal plots, and interpreted with principal component analysis [8] coupled with a interactive graphical system [9]. All specimen directions from a site or a handsample were averaged to obtain site or sample means. Since either a site or sample mean represents an independent record of the magnetic field (though, of course, the latter is not as precisely defined), it was decided to give an equal weight to each mean vector.

Wherever possible, the McFadden and Jones [10] fold test based on the mean directions of groups of sites with uniform bedding attitudes (referred here as the *M*-test) was performed for each locality separately; otherwise, the McElhinny [11] fold test, based on the Fisher precision parameter k (referred here as the *PP*-test) was used. During tectonic interpretation, flattening F and rotation R, and their confidence limits, were computed following Demarest [12].

4. Results

4.1. Overview

Intensities of natural remanent magnetization (NRM) usually range between 10^{-2} and 10^{-3} A/m. NRM directions concentrate in the northern half of the lower hemisphere, and display a better grouping after tilt correction than *in situ*. An unstable component of magnetization was usually removed by heating to 200 or 250°C. Above this temperature all samples revealed a well-defined component (A) of normal polarity which persisted up to as high as 670°C (Fig. 2). The unblocking temperature spectrum of this component is more or less uniform over the heating range, and it was reliably isolated from most specimens. It was often the only component which could be isolated (Figs. 2D and E). Its directions cluster well within each site or handsample.

The orthogonal plots often do not decay to the origin, and another linear trajectory may be recognized, thus implying the presence of another component (Figs. 2A and D). This component (B) can be isolated over a narrow temperature interval (650–680°C) and, when present, accounts for 10–20% of the NRM intensity (Fig. 2C). In some samples, component B could not be accurately determined, even if its presence was attested to

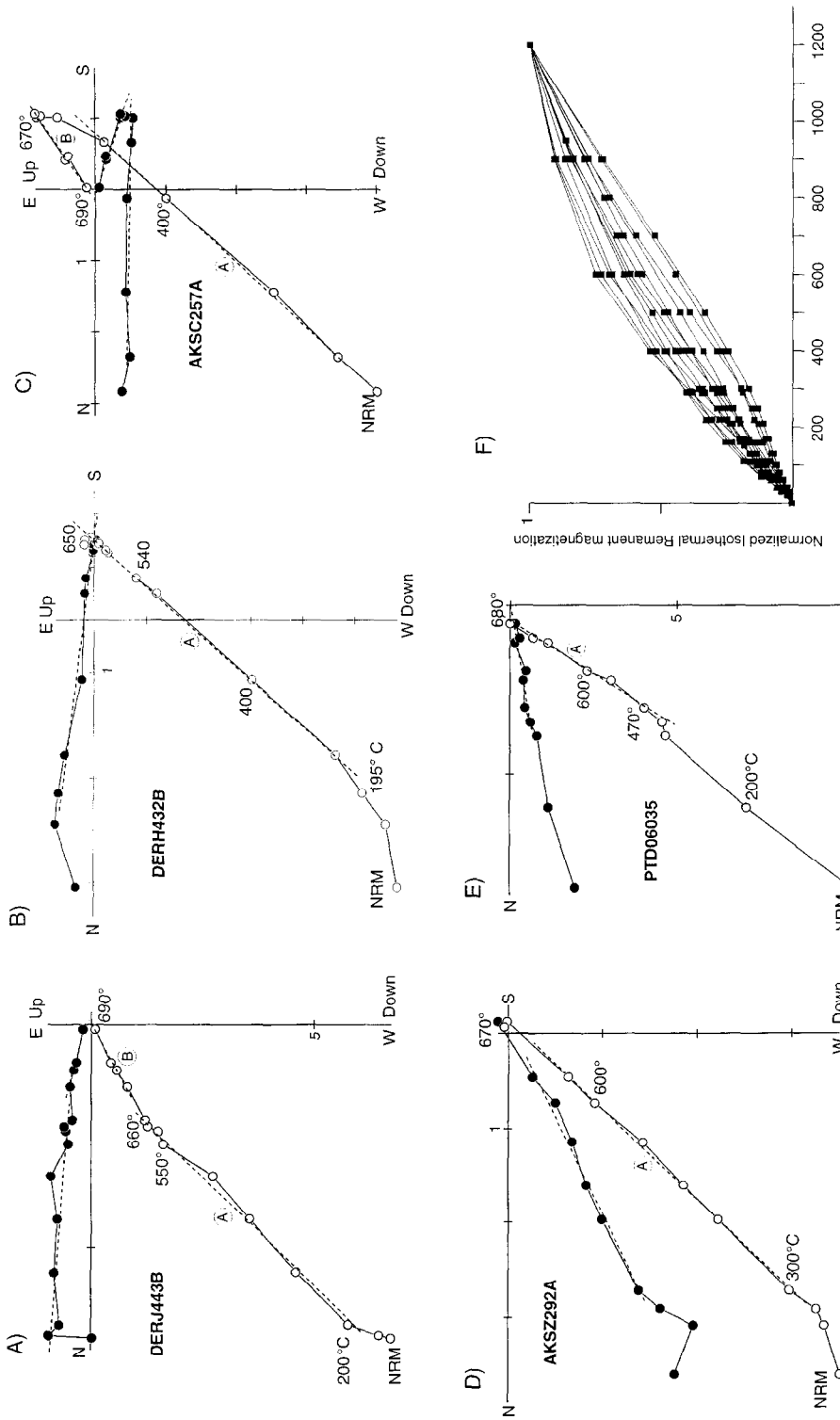

Fig. 2. (A–E) Representative orthogonal plots for Lower Cretaceous red beds from different localities. Dashed lines denote isolated components labelled A and B in the text. Data are plotted in stratigraphic coordinates (TC). ● = Vector end points projected onto the horizontal plane; ○ = vector end points projected onto the vertical plane. Steps are in degrees Celsius. (F) Isothermal remanent magnetization acquisition curves.

by demagnetization trajectories overshooting the origin (Figs. 2B and D).

NRM unblocking temperatures and isothermal remanent magnetization acquisition curves (Fig. 2F) point to hematite as the dominant carrier of magnetization.

4.2. The Derbent locality

Component A was reliably isolated from all fourteen sites (Table 1). Component B, adequately resolved from nine sites, is also of normal polarity. At still another site (DERH), component B is reversed, but it could not be accurately isolated there (Fig. 2B).

As demonstrated by the 95% positive *PP*-test, the clustering of site means after tilt correction is much better than *in situ* for both components (Tables 1 and 2 and Fig. 3). However, the *M*-test for component A yielded an **f**-statistic value larger than the critical value (Tables 1 and 2). A closer inspection of the data showed that the results from one of the limbs (sites DERA to DERC) differ both in declination and inclination from all the others, although these three sites are otherwise quite similar to the others. For the entire collection, the best data grouping ($k = 137$ and $k = 40$ for the components A and B, respectively) is achieved at about 80% unfolding. This, however, is entirely due to the same anomalous sites;

Table 1
Paleomagnetic directions of component A from the Derbent locality

Site	n/n_0	*In situ*				Tilt corrected			
		$D°$	$I°$	k	$\alpha_{95}°$	$D°$	$I°$	k	$\alpha_{95}°$
DERA	8/6	11	−11			33	58	149	6
DERB	7/6	1	−1			28	70	63	9
DERC	7/7	3	−11			33	73	253	4
DERD	8/8	323	6			14	52	238	4
DERE	7/7	332	12			3	50	274	4
DERF	8/8	328	20			6	53	81	6
DERG	9/9	26	71			358	50	297	3
DERH	9/9	33	66			4	47	159	4
DERI	9/9	19	56			358	46	469	2
DERJ	8/8	22	58			2	53	214	4
DERK	8/7	24	58			3	53	282	4
DERL	8/8	336	67			2	46	233	4
DERM	8/8	340	70			11	46	262	3
DERN	8/7	353	61			18	41	288	4
DERA-C	3	5	−8	112	8	32	67	102	8
DERD-F	3	328	13	95	8	8	52	443	4
DERG-K	5	24	62	141	5	1	50	465	3
DERL-N	3	344	66	153	7	11	44	158	6
All	14	356	40	5	17	9	53	52	5
$F(26,26) = 1.9$				$k_{tc}/k_{is} = 10.4$					
$F(6,20) = 2.6$		**f** = 95						**f** = 14.8	
DERD-N	11	351	53	8	15	6	49	193	3
$F(20,20) = 2.1$				$k_{tc}/k_{is} = 24.8$					
$F(4,16) = 3.0$		**f** = 74						**f** = 4.0	

* Statistics on the site-mean level. n/n_0 is number of specimens studied/used; D is declination, I inclination; k is Fischer precision parameter; α_{95} is radius of 95% confidence circle; F is 95% critical value of F distribution for the number of degrees of freedom in brackets; k_{tc}/k_{is} is the ratio of precision parameters after/before tilt correction; **f** is the calculated values of F statistics.

without them, the maximum is reached at 100% unfolding for both components. If we omit these three sites, the f-statistic value after tilt correction for component A decreases from 14.8 to 4, with a considerable improvement of the grouping of site means (Table 1). The latter value, however, is still slightly larger than the corresponding critical value (Table 1), but this is probably due to the limited number of sites.

4.3. The Aksu locality

Component A was reliably isolated from all sixteen sites (Table 3). Component B, adequately resolved from six sites, is bipolar (Table 4). As a rule, component B is no so well defined, but the general consistency of results is reasonable. Six specimens from the conglomerate yielded well-clustered directions close to the component A mean direction (Table 3).

Like at the Derbent locality, the *PP*-test is positive at the 95% level, but the *M*-test is negative for component A (Table 3 and Fig. 4). However, an analysis of the structural measurements shows that the fold axis of the anticline plunges about 20° northward, rendering incorrect a simple tilt correction. So, we corrected both bedding measurements and *in-situ* paleomagnetic directions for the axis plunge and, then, applied the common tilt correction to the thus-obtained bedding attitudes and remanence vectors [13]. With this two-stage unfolding algorithm, an excellent agreement of component A mean vectors from the three limbs was achieved, and the *M*-test became positive (Table 3 and Fig. 4). The grouping of component B is also improved when this algorithm is applied (Table 4 and Fig. 5). Moreover, after the two-stage correction, the maximum of the precision parameter for both components was achieved at 100% unfolding.

4.4. The Takob locality

Red beds from this locality behaved like those sampled at Derbent and Aksu, and a strong normal polarity component (A) was readily isolated here (Fig. 6). However, another component was adequately resolved from just a few specimens,

Table 2
Paleomagnetic directions of component B from the Derbent locality

Site	n/n_0	*In situ*				Tilt corrected			
		$D°$	$I°$	k	$\alpha_{95}°$	$D°$	$I°$	k	$\alpha_{95}°$
DERA	8/6	28	−14			47	44	40	11
DERB	7/5	5	−21			14	51	70	10
DERD	7/6	330	−1			5	44	21	15
DERE	7/7	338	−1			354	37	57	8
DERF	8/4	342	15			10	38	45	14
DERI	9/9	10	55			352	43	49	7
DERJ	8/8	16	43			4	37	42	9
DERM	8/6	7	56			17	28	91	7
DERN	8/7	357	50			14	31	62	8
Means *									
DERA-B	2	17	−18	–	–	32	49	–	–
DERD-F	3	334	4	53	11	3	40	119	7
DERI-J	2	13	49	–	–	358	40	–	–
DERM-N	2	2	53	–	–	16	29	–	–
All $F(16,16) = 2.3$	9	358	21	5	20 $k_{tc}/k_{is} = 6.4$	10	40	34	8
DERD-N $F(12,12) = 2.7$	7	351	32	8	19 $k_{tc}/k_{is} = 9.0$	6	37	72	6

See Table 1 for explanation.

and these data will not be used in the rest of our analysis. The grey sandstones were very weakly magnetized and yielded no meaningful results. Both fold tests point to a pre-folding age for component A (Table 5). The best grouping of data at 90% unfolding is just a few percent better than that for the tilt-corrected directions and is certainly statistically insignificant.

4.5. The South Darvaz locality

Only component A of normal polarity was isolated from eleven samples, and its tilt-corrected mean direction is very similar to the previously reported result (Table 5 and Fig. 7). Orthogonal plots for some samples slightly miss or bypass the origin, indicating the possible existence of a second unresolved component. The *PP*-test is not significant for this set of samples (Table 5), but these red beds were previously shown to have a pre-folding magnetization [4]. The best data grouping was achieved at 100% unfolding.

For several specimens of red beds from this locality, chemical leaching in hydrochloric acid revealed the same well-defined component that the thermal demagnetization revealed (Fig. 8). After removal of this component the paleomagnetic directions became erratic. Some leached and unleached specimens were isothermally magnetized up to 600 mT and then thermally demagnetized (Fig. 8). The IRM acquisition curves show that the leaching resulted in dissolution of high-coercitivity minerals which carry component A. High unblocking temperatures (up to 680°C) indicate that hematite is a carrier of component A. In the leached specimens, IRM is saturating in low fields, and unblocking temperatures are below 600°C. Magnetite can therefore be present in small proportions, and could carry the residual chaotic magnetization found at the final steps of chemical demagnetization.

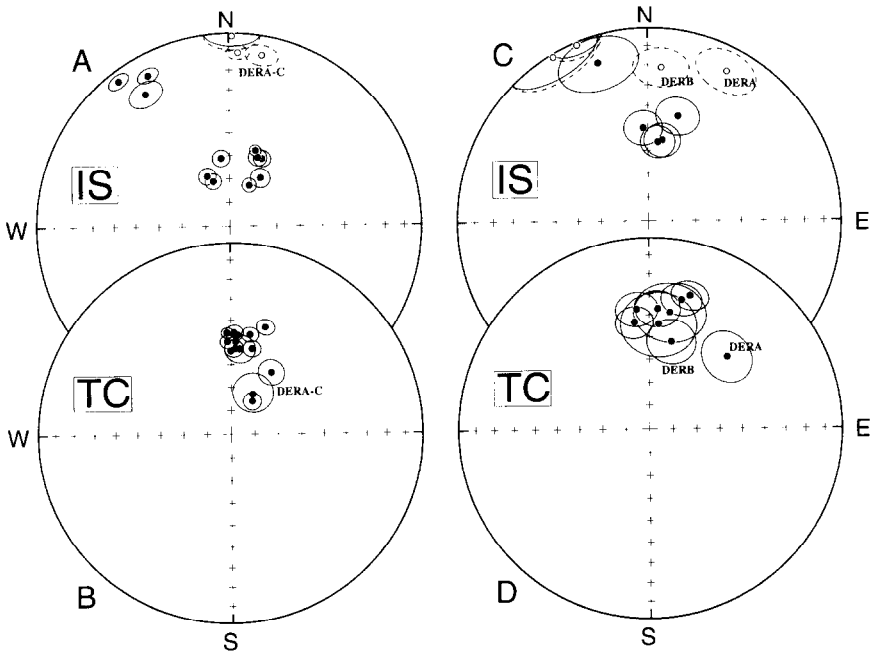

Fig. 3. Equal-area projection of site means of component A (A and B) and component B (C and D) fromthe Derbent locality, *in situ* (A and C) and after tilt correction (B and D). Solid symbols and solid lines are projected onto the lower hemisphere; open symbols and dashed lines are projected onto upper henisphere.

5. Data analysis

Component A of the ubiquitous normal polarity usually accounts for 80–90% of the NRM intensity. Judging by the orthogonal plots which often overshoot the origin, vector paths on stereonets, and the negative conglomerate test, this component is a secondary magnetization. As indicated by the leaching experiments, it seems to be carried by a hematite pigment which might have appeared in the red beds long after deposition, in accord to the conclusion of Pozzi and Feinberg [5] for the similar Lower Cretaceous red beds sampled in the northern and northeastern Tadzhik depression. Moreover, Lower Cretaceous red beds are widespread in the southern Tien Shan and the Fergana basin, and a similar overprint of normal polarity was found there too [14].

Pozzi and Feinberg [5] provided some evidence that a reverse high-temperature component is present in the Lower Cretaceous red beds, but they failed to isolate it. We were more lucky, mainly because we worked on a much larger collection, but even in our case component B was often isolated from just one or two specimens per site. In total, high-temperature bipolar component B has been found in less than a half of the collection. We blame the rather high within-site scatter of component B on the difficulty of isolating it from the short final parts of the orthogonal plots; a contamination by a stronger component A may also be present. Worth noting, however, is the fact that, in spite of high scatter, component

Table 3
Paleomagnetic directions of component A from the Aksu locality

Site	n/n_0	*In situ*				Tilt corrected				Unfolded			
		$D°$	$I°$	k	$\alpha_{95}°$	$D°$	$I°$	k	$\alpha_{95}°$	$D°$	$I°$	k	$\alpha_{95}°$
AKS4	8/7	73	34			343	53			0	53	166	5
AKS5	7/7	72	38			339	53			355	53	252	4
AKS6	7/7	72	33			344	51			2	51	186	4
AKS7	6/6	68	38			345	49			1	49	320	4
AKS8	6/6	59	39			334	44			351	44	953	2
AKS9	7/7	70	37			343	48			359	48	432	3
AKSZ	7/7	67	41			338	47			352	45	603	2
CONGL *	6/6	74	44			330	50			345	50	528	3
AKSA	7/7	308	46			21	52			10	52	44	9
AKSB	9/9	308	37			7	51			356	51	120	5
AKSC	7/7	306	37			5	53			354	53	191	4
AKSD	7/7	302	35			355	45			345	45	225	4
AKSE	9/9	307	33			355	41			346	41	263	3
AKSF	8/8	305	33			3	53			351	53	261	3
AKSG	7/7	359	65			2	52			2	52	257	4
AKSH	8/7	350	64			0	50			359	50	124	5
AKSI	7/7	352	62			0	48			0	48	459	3
Means **													
AKS4-9,Z	7	69	37	287	3	340	49	292	3	357	49	311	3
AKSA-F	6	306	37	235	4	4	49	102	6	353	49	106	6
AKSG-I	3	354	63	986	4	1	50	1408	2	0	50	1309	2
All	16	10	52	3		353	50	75	4	356	49	199	3
$F(4,26) = 2.7$			**f** = 489				**f** = 11.7				**f** = 0.7		

* Result from conglomerate was not used for calculation of mean.

** Statistics on the site-mean level. 'Unfolded' denotes results after the two-stage correction (see text); other notation as in Table 1.

Table 4
Paleomagnetic directions of component B from the Aksu locality

Site	n/n_0	*In situ*				Tilt corrected				Unfolded			
		$D°$	$I°$	k	$\alpha_{95}°$	$D°$	$I°$	k	$\alpha_{95}°$	$D°$	$I°$	k	$\alpha_{95}°$
AKS-5	7/5	62	35			347	46			3	46	27	15
AKS-9	7/7	188	−48			152	−3			168	−3	13	17
AKS-Z	7/5	192	−51			148	−7			165	−7	49	11
AKS-C	7/7	154	−35			193	−30			182	−30	16	16
AKS-F	8/4	162	−19			182	−17			171	−17	122	8
AKS-I	7/5	14	50			15	35			15	35	278	5
Mean *	6	7	44	9	24	352	24	11	22	356	23	17	17
$F(10,10) = 1.9$				$k_{tc}/k_{is} = 1.2$								$k_{uf}/k_{is} = 1.9$	

* All directions inverted to normal polarity. See Tables 1 and 3 for explanation.

B shows consistently lower inclination than component A, again in agreement with the Fergana results [14].

For the entire collections from the Derbent and Aksu localities, the best grouping of both components is achieved at an intermediate stage

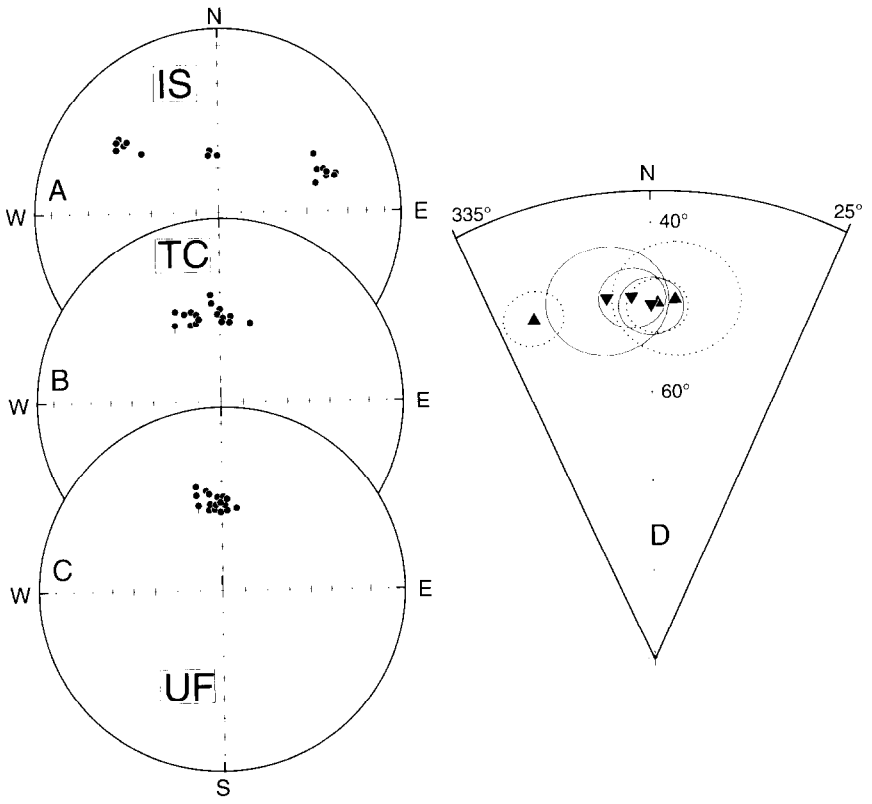

Fig. 4. Equal-area projection of site means (●) of component A from the Aksu locality *in situ* (A), after simple tilt correction (B) and after two-stage tilt correction as explained in the text (C). Dot with vertical tail = mean direction from a large block of conglomerate. Blow-up (D) shows mean directions together with associated confidence circles for each limb after simple tectonic correction (▲ and dotted lines) and two-stage correction (▼ and solid lines). All symbols are projected onto lower hemisphere.

of incremental unfolding. Such a pattern may be the result of several reasons, such as strongly overlapping unblocking spectra of post-folding and pre-folding components, complicated deformation style, synfolding remanence acquisition,

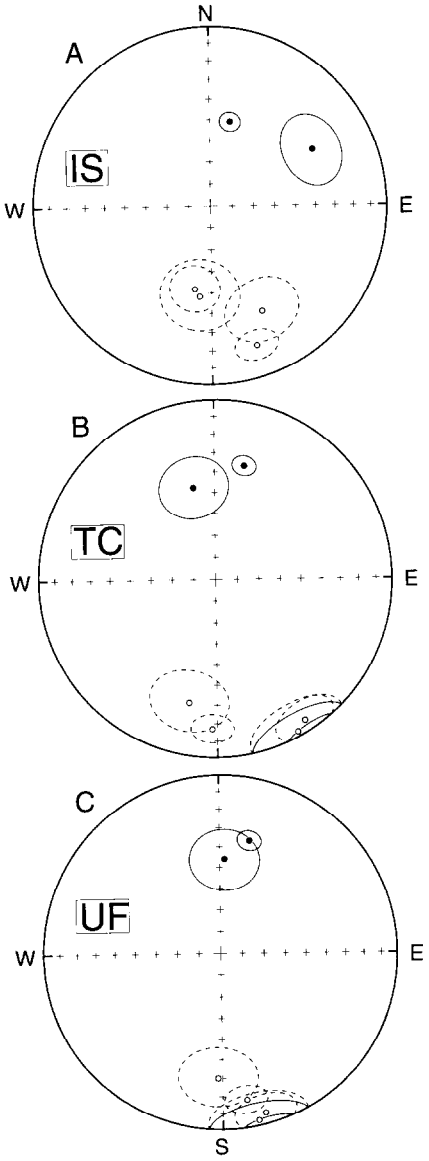

Fig. 5. Equal-area projection of site means (○ and ●) of component B from the Aksu locality *in situ* (A), after simple tilt correction (B) and after two-stage tilt correction as explained in the text (C). Solid symbols and solid lines are projected onto lower hemisphere; open symbols and dashed lines are projected onto upper hemisphere.

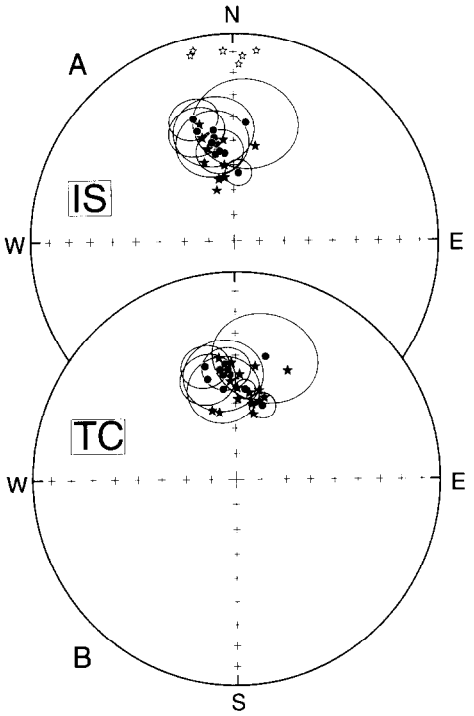

Fig. 6. Equal-area projection of site means (●) and sample means (☆ and ★) of component A from the Takob locality *in situ* (A) and after tilt correction (B). Solid symbols and solid lines are projected onto lower hemisphere; open symbols and dashed lines are projected onto upper hemisphere.

etc. We found no indication whatsoever of a pervasive post-folding component in the Lower Cretaceous red beds; hence, the first cause can be ruled out. The two-stage correction of the Aksu data led to an excellent agreement of site means for both components at 100% unfolding. The results from the Takob and South Darvaz localities are best grouped close to 100% unfolding, as are the Derbent data without the three anomalous sites DERA to DERC. Thus, only these three sites pose a problem. No deformation such as cleavage was noticed anywhere in the Lower Cretaceous rocks, and we cannot blame this anomaly on internal strain. Lower Cretaceous beds everywhere reveal clear and distinct bedding, and hence this cannot be a tilt-correction error. No sign of inclined fold axes was found at the Derbent locality. Most important, however, is the fact that any structural complexi-

ties should not affect inclinations while both components A and B at these sites are clearly steeper than the other directions (Tables 1 and 2). A synfolding hypothesis apparently fits the pattern but it is completely unclear how both components from these sites from a limited outcrop could have been synfolding while they are pre-folding everywhere else. In particular, absolutely 'normal' sites DERD to DERF are also from rather steeply dipping strata just a few hundred metres away from the outcrop where anomalous sites were sampled. At this stage, we cannot account for this anomaly, and the sites DERA to DERC were rejected.

As has already been stated, all the other data pre-date the deformation. The main folding and thrusting in this region is of Late Miocene age or even younger. However, close to the Oligocene–Miocene boundary, conglomerates up to several kilometres in thickness started accumulating in the basin, thus indicating a basin-and-range relief and therefore some tectonic activity. This is confirmed by Lower Miocene angular unconformities in the east of the Tadzhik basin [6]. In addition, angular unconformities of 10–15° between Upper Cretaceous and Paleocene strata have recently been reported [P.R. Cobbold, pers. commun., 1991]. The problem is the regional significance of the pre-Late Miocene unconformities, which are often considered to be local unconformities. With regard to the paleomagnetic data, the excellent agreement of component A directions at the Aksu, Takob and South Darvaz localities, and to lesser degree at the Derbent locality (Tables 1, 3 and 5), leads us to conclude that the remanence discussed above was acquired prior to any folding in the region. For the more dispersed component B, we can only conclude that the remanence pre-dates the main folding.

Although showing some lateral variability,

Table 5
Paleomagnetic directions of component A from the Takob and South Darvaz localities

Site	n/n_0	*In situ*				Tilt corrected			
		$D°$	$I°$	k	$\alpha_{95}°$	$D°$	$I°$	k	$\alpha_{95}°$
Takob									
TAK1	6/6	350	45			353	48	21	15
TAK2	6/6	341	44			344	48	41	11
TAK3	7/7	342	38			344	43	46	9
TAK4	6/6	348	50			352	54	25	14
TAK5	7/7	349	48			356	46	1008	2
TAK6	6/6	348	50			356	48	167	5
TAK7	7/7	348	55			353	47	281	4
TAK8	6/6	352	54			355	46	57	9
TAK9	6/5	6	42			14	39	17	19
TAK10	6/6	354	55			6	54	289	4
TAK11	6/5	4	63			20	59	219	5
HS-SL	12/10	350	57	59	6	9	52	72	5
HS-NL	13/6	357	−14	49	8	0	56	52	8
Mean *	27	352	40	8	10	2	52	60	4
$F(4,48) = 2.6$			**f** = 92				**f** = 1.0		
South Darvaz									
Mean	14/11	56	7	33	7	321	41	69	5
$F(20,20) = 2.1$				$k_{tc}/k_{is} = 2.1$					
Mean **	14/34					314	44	54	3
$F(4,62) = 2.5$			**f** = 8.5				**f** = 0.6		

* Same weight given to site means and sample means.
** Result and related statistics are from Bazhenov and Burtman [4]. HS-SL and HS-NL are handsamples from the southern and northern fold limbs respectively; see Table 1 for other notations.

Lower Cretaceous red beds are essentially the same from Amu-Darya River in the south, to the Tashkent area in the north, and to the eastern termination of the Fergana basin in the east. the paleomagnetic properties of these rocks are also similar throughout this region, with a large secondary component of normal polarity (component A) associated with a much weaker and less common high-temperature bipolar magnetization (component B). It does not seem likely that the acquisition of component A on a regional scale could have occurred in the Cenozoic, because this era was characterized by frequent changes in polarity. For this reason, we disagree with the Pozzi and Feinberg [5] hypothesis of a 40 Ma age for the normal polarity component. Instead, we infer the acquisition of the overprint during the Cretaceous quiet interval of normal polarity, which lasted from the Aptian up to the Santonian. An age of 95 Ma (the middle of the Cretaceous quiet interval) was arbitrarily assigned to component A.

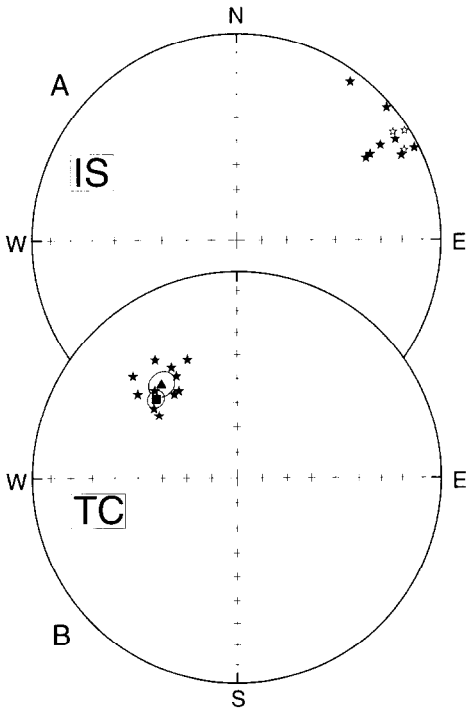

Fig. 7. Equal-area projection of sample means (☆and ★) from the South Darvaz locality *in situ* (A) and after tilt correction (B). ▲ = Mean direction of component A isolated from the completely demagnetized subset (see text); ■ = mean direction for the whole collection after heating to 400°C [4]. Solid symbols and solid lines are projected onto lower hemisphere; open symbols and dashed lines are projected onto upper hemisphere.

The bipolar character of component B agrees with the rock age (mainly pre-Aptian) and it may therefore be primary. But the systematically more gentle inclinations, both in the Tadzhik and Fergana basins, may be accounted for, for instance, by an inclination error or early diagenetic compaction. At the same time, we can compare component B to results from Oligocene–Lower Miocene red beds from the Aksu locality, which revealed a dual-polarity characteristic magnetization with a similar gentle inclination ($D = 347°$, $I = 33°$, $\alpha_{95} = 15°$, $N = 5$ sites [15]). Moreover, anomalously low inclinations in Eocene to Lower Miocene rocks have been reported from Kirghizia [16] and the peri-Pamir area [4], as well as from the other parts of the Alpine belt (for a review, see [17]). At present, we cannot rule out the possibility of a Cenozoic age for component B.

6. Interpretation and conclusions

The observed paleomagnetic inclinations and declinations from Tadzhikistan were compared with the Eurasian reference data (Fig. 9). Several versions of the mean Cretaceous pole for Eurasia have been proposed during the past decade. Khramov et al. [18] reported a mean pole for extra-Alpine Eurasia (within the former Soviet Union) for the entire Cretaceous. An Early Cretaceous pole for Eurasia was also calculated as an intersection of paleomeridians [19] in order to take into account the possibility that inclinations became more gentle, since the main body of data was from sediments. Mean Early and Late Cretaceous poles have been recomputed for Eurasia by Westphal et al. [17]. Still another version appeared in a new compilation of paleomagnetic data for Europe and North America [20]. The above mean poles were computed after application of different selection criteria to the available dataset. For instance, only two Early Cretaceous and three Late Cretaceous poles were used in the

last paper [20]. However, all these mean poles (referred to below as EA data) are rather consistent, and predict an inclination about 55° and declination about 20° (Fig. 9) for our area (reference point at 38.5°N, 68°E).

The reliability of the Eurasian Cretaceous dataset has recently been questioned, and an alternative apparent polar wander path (APWP) has been proposed [21]. For its Cretaceous part, just one Early Cretaceous and one Late Cretaceous pole from Europe remained, and three new ones from China and Korea were added. A master APWP was constructed by combining data from different continents. The reference directions for our area deduced from the master APWP (referred to below as BC data) predict systematically lower inclinations and more northerly declinations than those calculated from the EA poles (Fig. 9).

The internal consistency of our inclination data

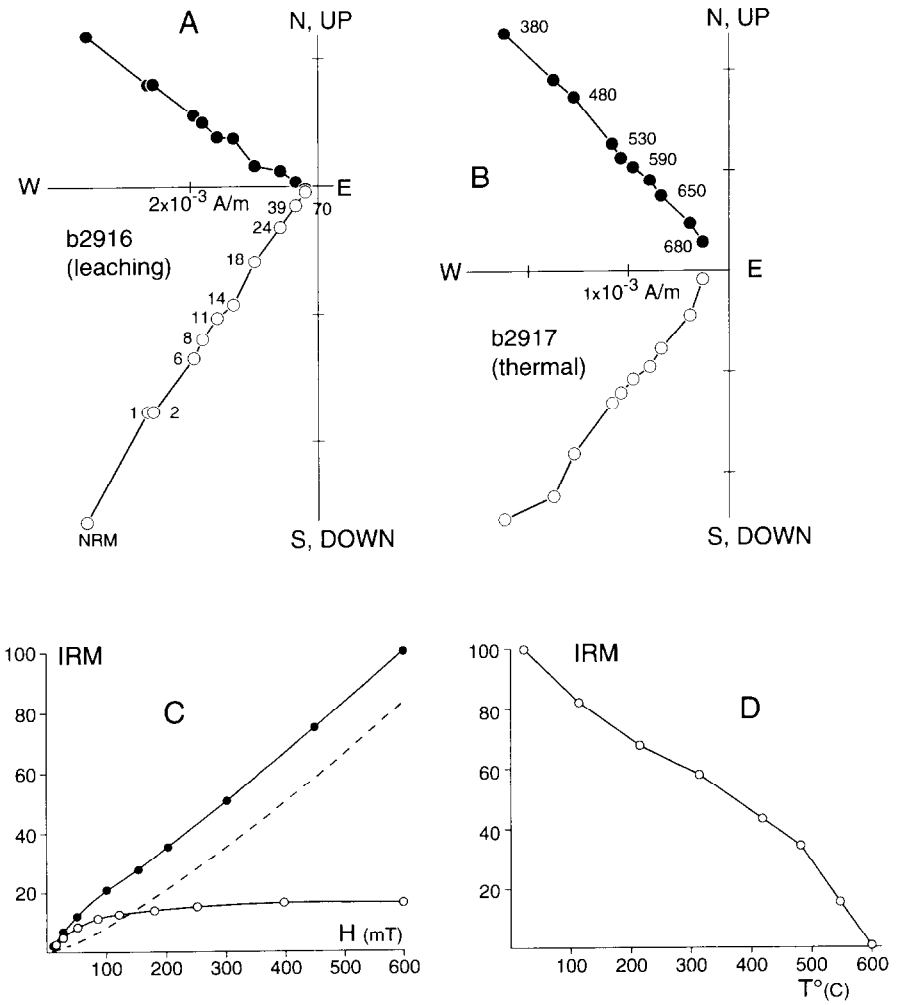

Fig. 8. Orthogonal plots for two samples from the South Darvaz locality subjected to chemical leaching (A) and thermal demagnetization (B). ● = Projections onto horizontal plane; ○ = projections onto vertical plane. Data are in stratigraphic coordinates. Steps are labelled in days (A) and degrees Celsius (B). (C) Isothermal magnetization curves for leached specimen (○) and unleached specimen from the same handsample. Dashed line is a would-be magnetization curve for magnetic phase removed by leaching (obtained by subtraction of two previous curves). (D) Thermal demagnetization of IRM for leached specimen.

for component A is very good: the Aksu, Derbent and Takob mean inclinations fall within 3° of each other. The South Darvaz result is several degrees more gentle but displaced in the correct sense if we were to take into account the northward push of this locality during the Pamir indentation into the Eurasian landmass and oroclinal bending of the External Pamir tectonic zone [4]. With respect to the EA reference inclinations, our results are systematically more gentle. In contrast, our data match well the BC expected inclinations, none of the measured flattening values being statistically significant; moreover, this good fit is almost independent of an age of component A acquisition provided that this age remains within the Cretaceous quiet interval (Fig. 9). Some shortening certainly took place in the Tien Shan during Alpine deformation, but it could hardly be much more than 200 km [22] and thus falls within the error limits. However, two mean inclinations of component B, and especially the Aksu result, are much lower than all the reference data. We believe that these large misfits in inclinations do not reflect tectonic movements but instead are due to peculiarities of this remanence acquisition (see above). Hence, we prefer not to use these results for the tectonic interpretation.

Unless a new major revision of the Eurasian APWP appears, declinations which are significantly below the BC reference declination curve (Fig. 9) are certainly from counterclockwise rotated localities (with respect to the BC data, all calculated rotations are conservative estimates and again almost independent of the component A age). The South Darvaz locality is clearly rotated counterclockwise ($R = 51 \pm 5°$) as the result of oroclinal bending of the Pamir arc [4]. The

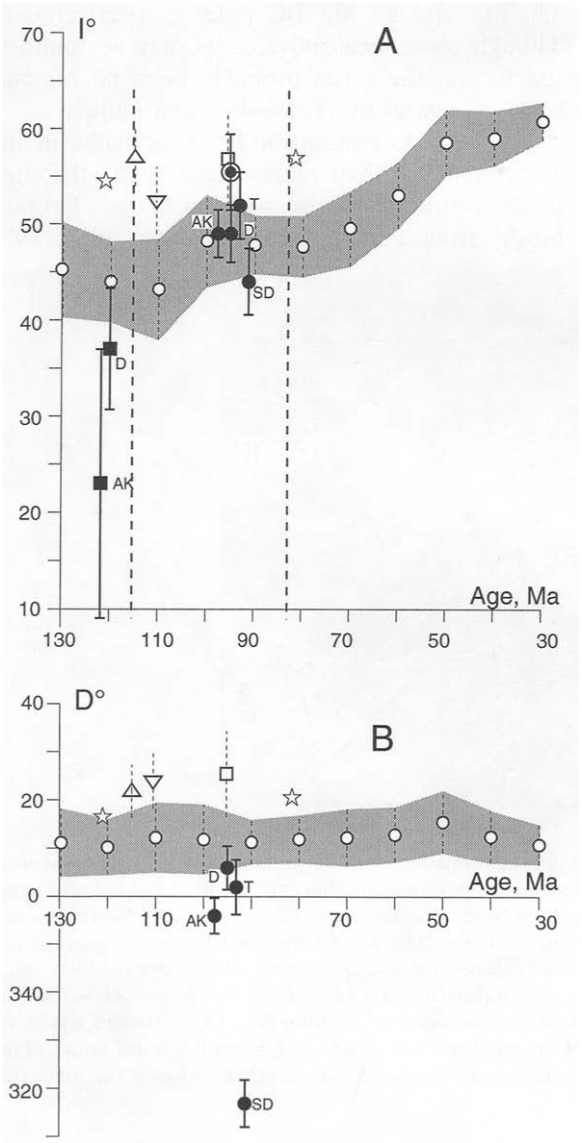

Fig. 9. Plots of inclination (A) and declination (B) versus age for Cretaceous data. ● and ■ = Our results for components A and B, respectively (*AK* = Aksu; *D* = Derbent; *T* = Takob; *SD* = South Darvaz). Encircled dot = overall mean from Pozzi and Feinberg [5]. Error bars are shown as solid lines. For clarity, our results are slightly displaced with respect to their presumed ages (95 Ma and 120 Ma for components A and B, respectively). ○ = Reference values from Besse and Courtillot [21], with associated confidence band (shaded). □, △, ▽ and ☆ = respectively Eurasian Cretaceous mean pole from Khramov et al. [18], Eurasian Early Cretaceous pole from Bazhenov and Shipunov [19], Eurasian Early Cretaceous pole from Westphal et al. [17] and European Early and Late Cretaceous poles from Van der Voo [20]. For reference date, error bars are shown as light dashed lines (for the data from Van der Voo [20] error bars are not shown because of the limited number of poles used). Thick dashed lines mark the boundaries of the Cretaceous quiet interval. Reference data are given the same ages as in the cited papers.

Aksu result from the inner part of the Tadzhik basin is also rotated in the same sense but through a much lesser angle (with respect to the 100 Ma BC pole, $R = 15 \pm 5°$). This finding is in accord with earlier results from the basin [3,5]. Mean declinations from the two localities on the periphery of the Tadzhik basin and southern Tien Shan, Derbent and Takob, differ significantly from the EA poles and less so from the BC data (Fig. 9). With respect to the 100 Ma BC direction the R-values are $5 \pm 5°$ and $9 \pm 6°$, respectively. At present, we consider the Derbent locality an unrotated part of Eurasia. For the Takob locality, the R-value is statistically significant, but close to the limits of paleomagnetically detectable rotations.

The pattern of paleomagnetic declinations of Cretaceous and younger rocks from the western part of the Tien Shan is rather consistent (Fig. 10). Both Cretaceous [this paper,14] and Paleogene [16] declinations west of the Talas–Fergana fault are systematically rotated counterclockwise, with the exception of a limited area close to the southern termination of the Talas–Fergana fault, where no rotations were found [14,23]. In contrast, the Issyk Kul and Naryn basins north of the same fault seem to be unrotated [16]. Further to the east, unrotated declinations were reported from Cretaceous and Tertiary rocks at the South Junggar basin–North Tien Shan boundary [24]. Finally, declinations in Upper Jurassic–Lower Cretaceous and Upper Cretaceous rocks from northern Tarim [25] agree well with the BC data (R-values are $7 \pm 11°$ and $2 \pm 10°$ with respect to 130 Ma and 90 Ma BC poles respectively). Al Though some local movements may be found in the future, there has probably been no regional rotation east of the Talas–Fergana fault.

Westerly declinations in the Fergana basin and adjacent Tien Shan ranges have been attributed to 25° counterclockwise rotation of the 'Fergana block' around an Euler pole at ca. 40°N, 69°E

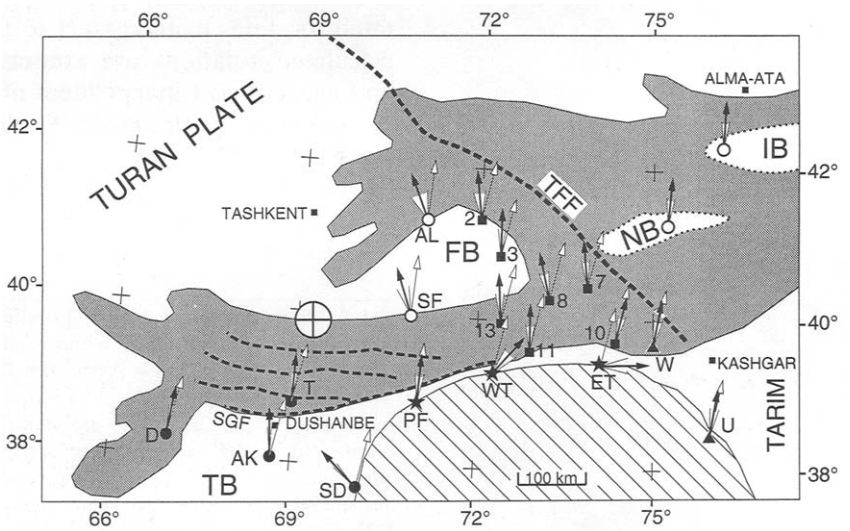

Fig. 10. Distribution of paleomagnetic declinations over the Pamirs (diagonal shading) and the western Tien Shan (grey shading). Black arrows = measured directions together with confidence angles shown as unfilled angles (it is not our fault that the confidence angles for some directions are difficult to see!). ● = Our data (*AK* = Aksu; *D* = Derbent; *T* = Takob; *SD* = South Darvaz); ■ = Cretaceous data from the Fergana basin and adjacent ranges numbered as in [14]; ▲ = Cretaceous data from Chen et al. [23] (*Y* = Uytak area; *W* = Wuqia area); ★ = Lower Cretaceous data from the external Pamir tectonic zone (*PF* = Peter the First range; *WT* = western Transalay range; *ET* = eastern Transalay range) [4]; ○ = Paleogene data (*IB* = Issyk Kul basin; *AL* = Alabuka; *SF* = south Fergana) [16]. White arrows = reference data recalculated from Besse and Courtillot [21]. Heavy dashed line is the Talas–Fergana fault (*TFF*); lighter dashed lines are major faults of the southern Tien Shan (*SGF* = south Ghissar fault). Major basins: *TB* = Tadzhik basin; *FB* = Fergana basin; *NB* = Naryn basin; *IB* = Issyk Kul basin. Large encircled cross is the Euler pole for the Fergana basin [16].

(Fig. 10) [14,16]. This choice was based on an analysis of the Alpine deformation pattern. In addition, it is the only permissible pole not leading to disruption of the Paleozoic tectonic zonation in the region. This Euler pole is not suitable for the new data from the Tadzhik basin, since it would imply a movement of the Tadzhik basin towards the Pamir wedge. We therefore consider that the Fergana and Tadzhik basins behaved as separate blocks during Alpine deformation.

Most geologists agree that Cenozoic deformation in Central Asia started in the late Oligocene–Early Miocene, its main part being of the Pliocene age. This Neogene tectonic activity is usually connected with the India–Eurasia collision. Our results show that the rotation is certainly post-Cretaceous in age. This conclusion is also confirmed by westerly declinations which we found in Oligocene–Miocene rocks from the Aksu locality, and the data of the same age reported from the South Darvaz area [15]. In general, the rotations deduced from the paleomagnetic results in the western part of the Tien Shan and Tadzhik basin fit the kinematic pattern as deduced from the structural and seismological data [2].

Acknowledgements

Thanks are due to the Academy of Sciences in Moscow and the CNRS in Paris for financial support, the French *Ministère des Affaires Etrangères*, and the University of Rennes and the University of Pau for their grants to M.B. We gratefully acknowledge F. Calza for assistance in the laboratory, S.V. Shipunov for permission to use his programs, and P.R. Cobbold for organizing the project.

References

[1] P. Tapponnier and P. Molnar, Active faulting and Cenozoic tectonics of the Tien Shan, Mongolia and Baikal region, J. Geophys. Res. 84, 3425–3459, 1979.

[2] P.R. Cobbold and P. Davy, Indentation tectonics in nature and experiment: 2. Central Asia, Bull. Geol. Inst. Univ. Uppsala, N.S. 14, 143–162, 1988.

[3] Kh.A. Abdullaev and Yu.S. Rzhevsky, Lower Cretaceous paleomagnetism of the Tadzhik basin, FAN, Tashkent, 1973 (in Russian).

[4] M.L. Bazhenov and V.S. Burtman, The Structural Arcs Of The Alpine Belt (the Carpathians, Caucasus, Pamirs), Nauka, Moscow, 1990 (in Russian).

[5] J.-P. Pozzi and H. Feinberg, Paleomagnetism in Tadzhikistan: continental shortening of the European margin in the Pamirs during Indian Eurasian collision, Earth Planet. Sci. Lett. 103, 365–378, 1991.

[6] V.A. Belsky, Recent tectonics of the boundary between the North Pamirs and Tadjik basin, Donish, Dushanbe, 1978 (in Russian).

[7] P.B. Baratov, ed., Stratified and Intrusive Formations of Tadzhikistan, Donish, Dushanbe, 1982 (in Russian).

[8] J.L. Kirschvink, The least-square line and plane and the analysis of palaeomagnetic data, Geophys. J.R. Astron. Soc. 62, 699–718, 1980.

[9] H. Perroud, Paléomagnétisme dans l'arc Ibéro-Armoricain et l'orogénèse varisque en Europe occidentale, Thesis, Univ. Rennes, 1985.

[10] P.L. McFadden and D.L. Jones, The fold test in palaeomagnetism, Geophys. J.R. Astron. Soc. 67, 53–58, 1981.

[11] M.W. McElhinny, Statistical significance of the fold test in palaeomagnetism, Geophys. J.R. Astron. Soc. 8, 338–340, 1964.

[12] H.H. Demarest, Jr., Error analysis for the determination of tectonic rotation from paleomagnetic data, J. Geophys. Res. 88, 4321–4328, 1983.

[13] N. Bonhommet, P.R. Cobbold, H. Perroud and A. Richardson, Paleomagnetism and cross-folding in a key area of the Asturian arc (Spain), J. Geophys. Res. 86, 1873–1887, 1981.

[14] M.L. Bazhenov, Cretaceous paleomagnetism of the Fergana basin and adjacent ranges, central Asia: tectonic implications, Tectonophysics 221, 251–267, 1993.

[15] J.-Ch. Thomas, A. Chauvin, D. Gapais, M.L. Bazhenov, H. Perroud, P.R. Cobbold and V.S. Burtman, Paleomagnetic evidence for Cenozoic block rotations in the Tadjik Deppression (Central Asia), J. Geophys. Res., in press, 1994.

[16] J.-Ch. Thomas, H. Perroud, P.R. Cobbold, M.L. Bazhenov, V.S. Burtman, A. Chauvin and E. Sadybokasov, A paleomagnetic study of Tertiary formations from the Kirgiz Tien Shan and its tectonic implications, J. Geophys. Res. 98, 9571–9589, 1993.

[17] M. Westphal, M.L. Bazhenov, J.P. Lauer, D.M. Pechersky and J.C. Sibuet, Paleomagnetic implications on the evolution of the Tethys belt from the Atlantic Ocean to the Pamirs from the Triassic, Tectonophysics 123, 37–82, 1986.

[18] A.N. Khramov, G.I. Goncharov, R.A. Komissarova, S.A. Pisarevsky, I.A. Pogarskaya, Yu.S. Rzhevsky, V.P. Rodionov and I.P. Slautsitais, Paleomagnetology, Nedra, Leningrad, 1982, (in Russian).

[19] M.L. Bazhenov and S.V. Shipunov, Paleomagnetism of Cretaceous rocks from Northern Eurasia: new results

and analysis, Izv. Akad. Nauk SSSR, Ser. Fiz. Zemli 6, 88–100, 1985 (in Russian).

[20] R. Van der Voo, Phanerozoic paleomagnetic poles from Europe and North America and comparisons with continental reconstructions, Rev. Geophys. 28, 167–206, 1990.

[21] J. Besse and V. Courtillot, Revised and synthetic apparent polar wander paths of the African, Eurasian, North American and Indian Plates and true polar wander paths since 200 Ma, J. Geophys. Res. 96, 4029–4050 1990.

[22] J.P. Avouac, P. Tapponnier, M. Bai, H. You and G. Wang, Active thrusting and folding along the Northern Tien Shan and late Cenozoic rotation of the Tarim relative to Dzungaria and Kazakhstan, J. Geophys. Res. 98, 6755–6804, 1993.

[23] Y. Chen, J.-P. Cogne and V. Courtillot, New Cretaceous paleomagnetic poles from the Tarim basin, Northwestern China, Earth Planet. Sci. Lett. 114, 17–38, 1992.

[24] Y. Chen, J.-P. Cogne, V. Courtillot, J.-Ph. Avouac, P. Tapponnier, G. Wang, M. Bai, H. You, M. Li, C. Wei and E. Buffetaut, Paleomagnetic study of Mesozoic continental sediments along the Northern Tien Shan (China) and heterogeneous strain in Central Asia, J. Geophys. Res. 96, 4065–4082, 1991.

[25] Y.P. Li, Z.K. Zhang, M. McWilliams, R. Sharps, Y.J. Zhai, Y.A. Li, Q. Li and A. Cox, Mesozoic paleomagnetic results of the Tarim craton: Tertiary relative motion between China and Siberia?, Geophys. Res. Lett. 15, 217–220, 1988.